ARTICLE

An Asymmetrically Surface-Modified Graphene Film Electrochemical Actuator

Xuejun Xie,[†] Liangti Qu,[†,*] Ce Zhou,[†] Yan Li,[†] Jia Zhu,[‡] Hua Bai,[§] Gaoquan Shi,[§,*] and Liming Dai[⊥,*]

[†]Key Laboratory of Cluster Science (Beijing Institute of Technology), Ministry of Education of China, School of Science, Beijing Institute of Technology, Beijing 100081, P. R. China, [‡]College of Chemistry, Beijing Normal University, Beijing 100875, P. R. China, [§]Department of Chemistry, Tsinghua University, Beijing 100084, P. R. China, and [⊥]Department of Chemical Engineering, Case School of Engineering, Case Western Reserve University, Cleveland, Ohio 44106

ABSTRACT It is critically important to develop actuator systems for diverse needs ranging from robots and sensors to memory chips. The advancement of mechanical actuators depends on the development of new materials and rational structure design. In this study, we have developed a novel graphene electrochemical actuator based on a rationally designed monolithic graphene film with asymmetrically modified surfaces. Hexane and O_2 plasma treatment were applied to the opposite sides of graphene film to induce the asymmetrical surface properties and hence asymmetrical electrochemical responses, responsible for actuation behaviors. The newly designed graphene actuator demonstrated here opens a new way for actuator fabrication and shows the potential of graphene film for applications in various electromechanical systems.

KEYWORDS: graphene · actuator · asymmetrical modification · electrochemistry

*Address correspondence to lqu@bit.edu.cn, gshi@tsinghua.edu.cn, liming.dai@case.edu.

Received for review July 7, 2010 and accepted September 1, 2010.

Published online September 9, 2010. 10.1021/nn101563x

It is very important to develop advanced actuators for diverse applications ranging from robots to sensors to memory chips.[1−4] In this regard, various conducting polymer[5,6] and carbon nanotube (CNT)[7,8] based actuators have been developed for reversible control of mechanical motions. Unlike conducting polymer actuators that operate by Faradaic doping and undoping, CNT actuators are non-Faradaic and directly driven by electrical charging and discharging.[7,8] Although a few of unimorph actuators with a single layer configuration have been demonstrated,[9−11] most actuators reported previously consist of a bilayer or multilayer architecture.[5−8]

As a building block for carbon nanotubes and other carbon nanomaterials, the two-dimensional (2-D) single atomic carbon sheets of graphene have recently attracted tremendous research interest due to their large surface area, high carrier transport mobility, superior mechanical flexibility, and excellent thermal/chemical stability.[12−15] As a consequence, an attempt has been made to fabricate nanoelectromechanical resonators based on a single or few-layer graphene sheets.[16] It has been reported that graphene or its oxides could be used as filler of composite film for actuators.[17,18] Recently, a macroscopic assembly of graphene oxide and multiwalled CNT (MWCNT) bilayer paper demonstrated interesting humidity and/or temperature-dependent actuation (curling) behaviors.[19] However, the general application of the graphene oxide in electrically driven actuator devices is precluded by the electrical insulation nature of graphene oxides. Herein, we present a newly designed unimorph electrochemical actuator based on a monolithic graphene film with asymmetrically (Asy-) modified surfaces.

RESULTS AND DISCUSSION

The graphene film (Figure 1a) is made by direct filtration of an aqueous suspension of reduced graphene oxide colloids. An appropriate thickness of 4−5 μm was chosen for a free-standing, mechanically flexible but not stiff graphene film for actuator investigation. Both sides of the as-prepared graphene film have similar surface characteristics as confirmed by scanning electron microscopic (SEM), X-ray diffraction (XRD), and water contact angle measurements (Supporting Information Figures S1−S3). The as-prepared graphene film in this study (Figure 1a) has an interlayer spacing of ~0.374 nm (Supporting Information, Figure S1), larger than that of common graphite plate (~0.34 nm). The relatively large interlayer distance provides additional advantages for accessibility to electrolyte and makes the graphene layers more movable. To change the surface properties asymmetrically, we treated one side of the graphene film with hexane plasma (Hex−P), followed by exposure of the other side to O_2 plasma (O_2−P) (Figure 1b). The Hex−P treatment enhanced the surface hydrophobicity (Figure 1b, left inset) and provided the effective protection of graphene

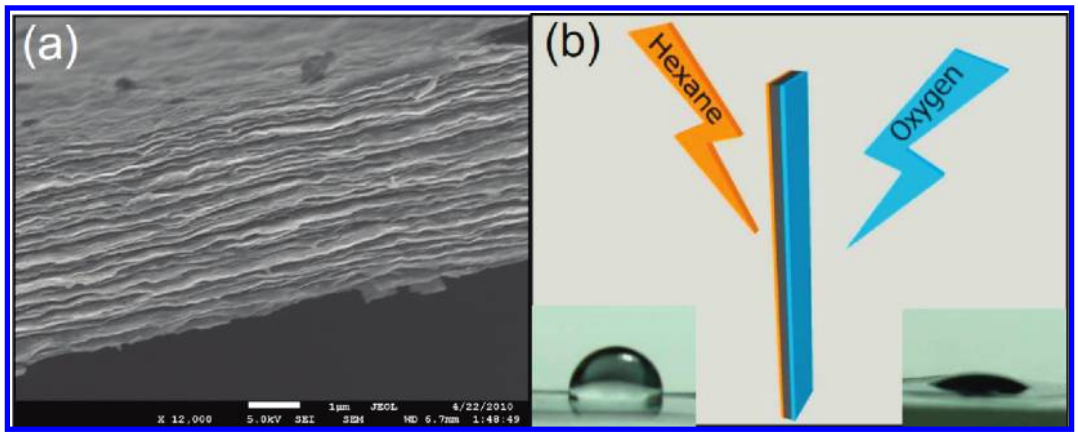

Figure 1. (a) Cross-section SEM image of a graphene film (scale bar: 1 μm). (b) Illustration of asymmetric plasma treatments of the graphene film with hexane and oxygen, and the corresponding surface wettabilities. Water contact angles for the Hex−P (b, left inset) and O_2−P (b, right inset) treated surfaces are ~90° and ~15°, respectively.

surface from the accessibility of electrolyte ions, which accordingly weakened the surface electrochemical response as demonstrated below in Figures 4 and 5. The O_2−P treated surface became very hydrophilic (Figure 1b, right inset) and readily accessible to aqueous media due to the plasma-induced oxygen-containing groups.[20−22] The asymmetric surface properties of graphene film will induce the distinction of electrochemical response, which produces the driving force responsible for the actuation behavior.

It is notable that the O_2−P treated graphene film is different from graphene oxide (GO) film. Although GOs are also hydrophilic and can be a film by filtration, the intrinsically electrical insulation could be the kittle obstacle for development of electrically driven actuators. In contrast, graphene sheets after O_2−P treatment still possess superior electric conductance facilitating the actuator application. On the other hand, GOs are dispersible in aqueous solution due to oxygen-containing functional groups rich on their surfaces, which will cause the structure damage of GO film during actuation investigation in aqueous electrolyte. Unlike the GO film, the O_2-plasma treated graphene film can remain the intact structure in aqueous medium because the oxygen-containing groups merely cover the surface of graphene film.

To demonstrate actuation action, a cut strip of the Asy-modified graphene film (2 mm by 20 mm) was used as working electrode. Pt wire and Ag/AgCl were used as counter-electrode and reference electrode in a single electrochemical cell. When the Asy-modified graphene strip was immersed into the aqueous 1 M $NaClO_4$ electrolyte, a slight surface curling toward the Hex−P treated side occurred due to the swelling of the O_2−P treated surface by the aqueous electrolyte. Upon cyclic voltammogramic (CV) scanning within the potential region of ±1.2 V (Figure 2), the graphene strip showed a deflection up to about 15 mm at the strip tip, which reversed on reversal of the applied potential (Supporting Information, video). We used the mean curvature of the Asy-modified graphene strip to quantify the actuation response (Figure 2 and Scheme S1). Each point represents an equilibrium state at a certain CV potential in Figure 2. As can be seen, the graphene strip bends to the Hex−P treated side at negative voltages (Figure 2, left inset) and to the O_2−P treated side under a positive applied potential (Figure 2, right inset). The bending degree of the graphene strip increased with increasing intensity of the applied voltage under both the positive and negative bias. However, at higher potential (>1.0 V), a saturated curvature of *ca.* 0.6 cm^{-1} appeared probably due to the rigidity of the graphene strip. The asymmetric surface properties are crucial for the reversible actuation behavior of the graphene film. The untreated graphene film and the one with its both sides treated by Hex−P or O_2−P display negligible movement under the same CV scan due to the indistinguishable surface properties.

Square wave potentials were applied to investigate the effect of scan frequency on the performance of the graphene actuator. As is the case for CNT actuators,[7,23] the graphene actuator exhibited large curvature at relatively low frequency (Figure 3a). The observed decrease in the curvature of the graphene actuator with increasing scan frequency is due to the insufficient charging time at a high frequency. As shown in Figure

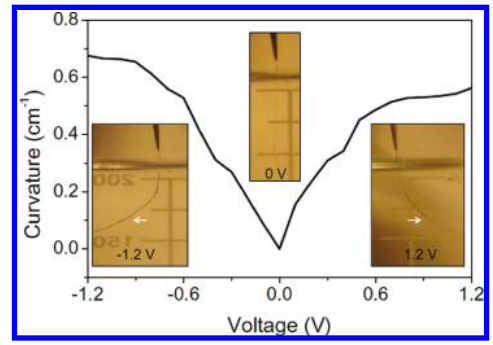

Figure 2. Curvature change of an Asy-modified graphene strip as a function of applied CV potential within ±1.2 V. Insets show the status of the graphene strip at −1.2, 0, and 1.2 V, respectively.

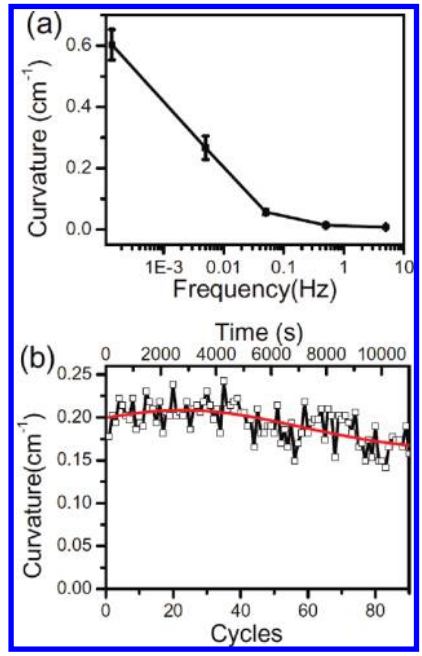

Figure 3. (a) Curvature of the graphene actuator as a function of frequency at applied square wave voltage of 1.2 V, and (b) the durability at a frequency of 0.01 Hz.

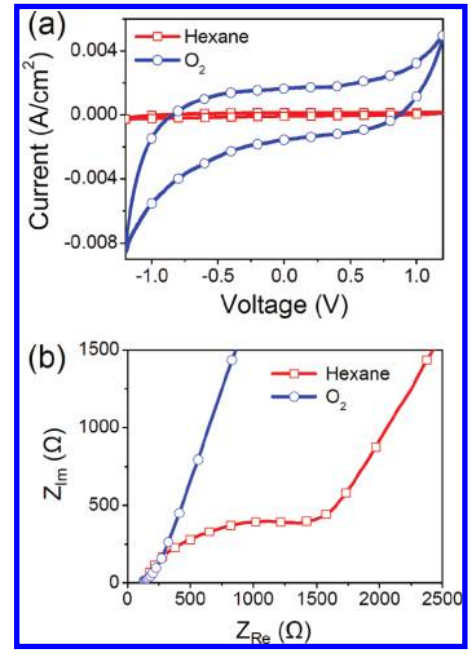

Figure 4. CV curves (a) and Nyquist plots (b) for the Hex−P and O_2−P treated graphene films in aqueous $NaClO_4$ solution.

3b, the curvature of the graphene actuator decreased only by *ca.* 10% over 90 measurement cycles (*ca.* 3 h), indicating a fairly stable actuation response for the graphene actuator.

Raman spectra show neither structural damage nor defect during the actuation process (Supporting Information, Figures S4 and S5). However, SEM images reveal that slight wrinkles were formed on the actuator surfaces due to continuously reversible bending, though the layer-by-layer structure was retained for the graphene actuator (Supporting Information, Figure S6). XRD analyses indicate an increased interlayer distance in the graphene film caused by the charging/discharging process associated with the actuation response (Supporting Information, Figure S7). Particularly, the *d* spacing for the original graphene film (0.374 nm) slightly increased to 0.378 and 0.381 nm for the Hex−P and O_2−P treated surfaces, respectively, after the repeated actuation bending. A little bigger value of *d* spacing for the O_2−P treated surface compared with the Hex−P treated side indicates that the O_2−P treated surface is more active in response to the electrochemical process. These results may also imply that the electrolyte could intercalate into the interlayers of graphene sheets leading to increased interlayer spacing during charging/discharging and actuation process.

Owing to the intrinsically structural similarity of CNTs and graphene sheets, it is reasonable to speculate that the graphene actuator works mainly *via* the non-Faradaic electrical charging/discharging analogous to the CNT-based actuators.[7,23,24] In fact, it has been previously predicated that a plannar graphite sheet possessed the electrostrictive effect similar to that of CNTs.[25] For the Asy-modified graphene film, the difference in electrochemically induced charge injections into the plasma/graphene interfaces at the two opposite sides could result in the deformation of the graphene film.

The asymmetric response of the opposite sides for the Asy-modified graphene film was further confirmed by electrochemical investigation. As shown in Figure 4a, the CV response of the O_2−P treated graphene film presents a significantly enhanced capacitive loop compared with that of the Hex−P treated one. The areal capacitance (C_A) for the O_2−P treated graphene film is estimated to be 2.83 mF/cm^2, whereas the C_A for the Hex−P treated graphene film is only 0.05 mF/cm^2. These results indicate the ability for charge accumulation in the electrode−electrolyte interface for the O_2−P treated graphene film is much higher than that of the Hex−P treated counterpart. The electrochemical impedance spectroscopy (EIS) was also carried out to investigate the kinetics of ion exchange in the interface of the graphene film and electrolyte solution, which was directly responsible for the actuator performance to some extent. Figure 4b illustrates the Nyquist plots of the Hex−P and O_2−P treated graphene films. Good electrical conductivity and rapid charge transfer at the electrode−electrolyte interface was revealed for the O_2−P treated graphene film, while finite ion diffusion was observed for the Hex−P treated counterpart. The EIS of Figure 4b could be modeled by the simple equivalent circuit (Supporting Information, Figure S8). The values of nonlinear curve-fitting show that double layer capacitance for O_2−P treated graphene film (1.1 mF/cm^2) is 2 orders of magnitude higher than that of

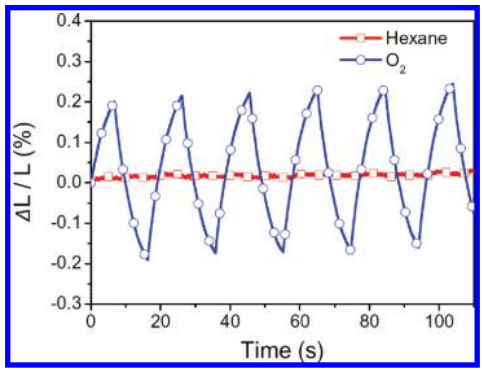

Figure 5. The length changes of the graphene strips treated with Hex−P and O_2−P under applied square wave potential of ±1.2 V with a frequency of 0.05 Hz (*L* and Δ*L* are defined as the length and length change of graphene actuator).

Hex−P treated one (2.2×10^{-2} mF/cm^2), which is consistent with the measured areal capacitance mentioned above. In the meanwhile, the charge transfer resistance for the O_2−P treated graphene film is only 7×10^{-2} Ω/cm^2, much lower than that of the Hex−P treated counterpart (2.7×10^3 Ω/cm^2). These results, once again, indicate that the O_2−P-treated graphene film possesses superior ability for charge accumulation and transfer compared with its Hex−P treated counterpart. High capacitance could facilitate the charge injection to and C−C bond expansion of the graphene sheet at the interface.

We also quantitatively investigated the length changes of graphene strips treated solely with Hex−P and O_2−P under applied square wave potentials. Similar to the case of a CNT actuator,[7] the electron injection into a graphene sheet electrode could cause an expansion, while a contraction occurred for the hole injection process. As shown in Figure 5, the O_2−P treated graphene strip displayed a rhythmic length change up to 0.2% in response to the potential change, while the Hex−P treated one exhibited a noise-like fluctuation. The length change for the O_2−P treated graphene strip is about 20−50 times larger than that of its Hex−P treated counterpart. Although the exact actuation mechanism of the graphene actuator needs further study, the asymmetric surface properties of the Asymodifed graphene film seem to play a crucial role in regulating electromechnical behaviors of the film surfaces and controlling the overall motion of the graphene actuator.

CONCLUSIONS

A newly designed graphene film actuator has been demonstrated by asymmetric surface modification of the two opposite sides of the monolithic graphene film with the hexane and O_2 plasma, respectively, which induced the actuation motion through asymmetric electrochemical charging and discharging. Although the achieved response frequency is relatively low in this primary study, the actuator performance could be enhanced by the reconstruction of the actuator configuration, introduction of nano/microscale porous structures, and functionalization/modification of graphene sheets. By increasing the surface area of graphene film and the accessibility to electrolyte, the charge/discharge speed, as well as the capacitance, will be largely improved. The promising actuation behaviors demonstrated for the unoptimized graphene actuator developed here indicate that the graphene-based actuator holds great potential for applications in various electromechanical systems.

METHODS

Graphite oxide was prepared from natural graphite powder *via* acid-oxidation according to a modified Hummers method reported in our previous paper.[26] Reduction of the graphene oxide was then carried out with aqueous N_2H_4 in the presence of ammonia. Briefly, 2 mL of 0.2 mg/mL graphene oxide was treated with 200 μL of concentrated ammonium hydroxide (NH_4OH) and ~15 μL of hydrazine monohydrate ($N_2H_4 \cdot H_2O$) for 1 h at 90 °C. The freestanding graphene film was made by direct filtration of the aqueous reduced graphene oxide colloidal suspensions through a filter membrane with a pore size of 220 nm. The dried graphene film with a thickness of *ca.* 4−5 μm was mechanically peeled from the filter. The measured conductivity is *ca.* 1×10^3 S/m, a value better than that of pyrenebutyrate-functionalized graphene films.[26] This freestanding graphene film composed of layer-by-layer graphene sheets, without further optimization of its mechanical strengths, surface characteristics, or electrical properties, was used for subsequent fabrication of the graphene actuator.

Plasma treatment was carried out on a custom-built plasma apparatus powered at 13.56 MHz, 200 W (Cesar 133 RF power generator) and a pressure of 100 Pa with hexane or O_2 flow. The plasma was applied for less than 10 s in order to avoid possible surface damage of the graphene film.

Actuation behavior was investigated in a three-electrode one-cell system with a cut strip of graphene film (2 mm × 20 mm) and Pt wire being used as the actuator electrode and counter-electrode, respectively. Electrolyte is the aqueous solution 1 M $NaClO_4$. All of the electrochemical measurements in this study were carried out by using Ag/AgCl as a reference electrode. Cyclic voltammetry was performed at a scan rate of 10 mV/s. Nyquist plots were obtained by using the plasma treated graphene films as a working electrode with an amplitude of 5 mV, frequency ranging from 0.5 to 10^6 Hz, and a DC cell potential of 1 V.

The bending degree of the graphene actuator is quantitatively expressed by the curvature, which is dependent on both the length and displacement of the graphene strip, and directly proportional to the bending degree of the graphene actuator (Supporting Information, Scheme S1). The deformation of graphene actuator was recorded by virtue of the method mentioned in ref 24 with the assistance of a camera (Canon EOS 1000D) to continuously image the graphene actuator. The displacement can also be directly calculated from the taken images. The length change of the graphene strips was measured using a similar setup presented in ref 23 with a lab-made laser displacement system, where the CNT tower was replaced with the graphene strip (Supporting Information, Figure S9).

The electrochemical measurements of the graphene film were performed by the use of a CHI660D electrochemical workstation. The morphology of the samples was examined by scanning electron microscopy (SEM, JSM-7500F). X-ray diffraction

(XRD) patterns were obtained by using a Netherlands 1710 diffractometer with graphite monochromatized Cu Kα irradiation (μ = 1.54 Å). Raman spectra were recorded using a RM 2000 microscopic confocal Raman spectrometer (Renishaw PLC, England) under an Ar ion laser with an excitation wavelength of 514.5 nm.

Acknowledgment. This work was supported by BIT, the 111 Project B07012 in China, and the program for the new century excellent talents in University (NCET). L. Dai is grateful for the support from NSF (CMS-0609077).

Supporting Information Available: Structure, surface properties, and actuation studies of graphene actuators (Figures S1−S9, Scheme S1, and Video S1). This material is available free of charge *via* the Internet at http://pubs.acs.org.

REFERENCES AND NOTES

1. Kim, P.; Lieber, C. M. Nanotube Nanotweezers. *Science* **1999**, *286*, 2148–2150.
2. Ahir, S. V.; Terentjev, E. M. Photomechanical Actuation in Polymer Nanotube Composites. *Nat. Mater.* **2005**, *4*, 491–495.
3. Fennimore, A. M.; Yuzvinsky, T. D.; Han, W. Q.; Fuhrer, M. S.; Cumings, J.; Zettl, A. Rotational Actuators Based on Carbon Nanotubes. *Nature* **2003**, *424*, 408–410.
4. Jang, J. E.; Cha, S. N.; Choi, Y. J.; Kang, D. J.; Butler, T. P.; Hasko, D. G.; Jung, J. E.; Kim, J. M.; Amaratunga, G. A. J. Nanoscale Memory Cell Based on a Nanoelectromechanical Switched Capacitor. *Nat. Nanotechnol.* **2007**, *3*, 26–30.
5. Jager, E. W. H.; Smela, E.; Inganas, O. Microfabricating Conjugated Polymer Actuators. *Science* **2000**, *290*, 1540–1545.
6. Lu, W.; Fadeev, A. G.; Qi, B.; Smela, E.; Mattes, B. R.; Ding, J.; Spinks, G. M.; Mazurkiewicz, J.; Zhou, D.; Wallace, G. G. Use of Ionic Liquids for π-Conjugated Polymer Electrochemical Devices. *Science* **2002**, *297*, 983–987.
7. Baughman, R. H.; Cui, C.; Zakhidov, A. A.; Iqbal, Z.; Barisci, J. N.; Spinks, G. M.; Wallace, G. G.; Mazzoldi, A.; De Rossi, D.; Rinzler, A. G. Carbon Nanotube Actuators. *Science* **1999**, *284*, 1340–1344.
8. Qu, L. T.; Peng, Q.; Dai, L. M.; Spinks, G. M.; Wallace, G. G.; Baughman, R. H. Carbon Nanotube Electroactive Polymer Materials: Opportunities and Challenges. *MRS Bull.* **2008**, *33*, 215–224.
9. Sansinena, J. M.; Gao, J.; Wang, H. L. High-Performance, Monolithic Polyaniline Electrochemical Actuators. *Adv. Funct. Mater.* **2003**, *13*, 703–709.
10. Han, G.; Shi, G. Electrochemical Actuator Based on Single-Layer Polypyrrole Film. *Sens. Actuat. B* **2006**, *113*, 259–264.
11. Baker, C. O.; Shedd, B.; Innis, P. C.; Whitten, P. G.; Spinks, G. M.; Wallace, G. G.; Kaner, R. B. Monolithic Actuators from Flash-Welded Polyaniline Nanofibers. *Adv. Mater.* **2008**, *20*, 155–158.
12. Geim, A. K. Graphene: Status and Prospects. *Science* **2009**, *324*, 1530–1534.
13. Stankovich, S.; Dikin, D. A.; Dommett, G. H. B.; Kohlhaas, K. M.; Zimney, E. J.; Stach, E. A.; Piner, R. D.; Nguyen, S. B. T.; Ruoff, R. S. Graphene-Based Composite Materials. *Nature* **2006**, *442*, 282–286.
14. Eda, G.; Fanchini, G.; Chhowalla, M. Large-Area Ultrathin Films of Reduced Graphene Oxide as a Transparent and Flexible Electronic Material. *Nat. Nanotechnol.* **2008**, *3*, 270–274.
15. Blake, P.; Brimicombe, P. D.; Nair, R. R.; Booth, T. J.; Schedin, F.; Ponomarenko, L. A.; Morozov, S. V.; Gleeson, H. F.; Hill, E. W.; Geim, A. K. Graphene-Based Liquid Crystal Device. *Nano Lett.* **2008**, *8*, 1704–1708.
16. Bunch, J. S.; van der Zande, A. M.; Verbridge, S. S.; Frank, I. W.; Tanenbaum, D. M.; Parpia, J. M.; Craighead, H. G.; McEuen, P. L. Electromechanical Resonators from Graphene Sheets. *Science* **2007**, *315*, 490–493.
17. Liang, J. J.; Xu, Y. F.; Huang, Y.; Zhang, L.; Wang, Y.; Ma, Y. F.; Li, F. F.; Guo, T. Y.; Chen, Y. S. Infrared-Triggered Actuators from Graphene-Based Nanocomposites. *J. Phys. Chem. C* **2009**, *113*, 9921–9927.
18. Lian, Y. F.; Liu, Y. X.; Jiang, T.; Shu, J.; Lian, H. Q.; Cao, M. H. Enhanced Electromechanical Performance of Graphite Oxide−Nafion Nanocomposite Actuator. *J. Phys. Chem. C* **2010**, *114*, 9659–9663.
19. Park, S.; An, J.; Suk, J. W.; Ruoff, R. S. Graphene-Based Actuators. *Small* **2010**, *6*, 210–212.
20. Lu, W.; Qu, L. T.; Henry, K.; Dai, L. M. High Performance Electrochemical Capacitors from Aligned Carbon Nanotube Electrodes and Ionic Liquid Electrolytes. *J. Power Sources* **2009**, *189*, 1270–1277.
21. Seo, M. K.; Park, S. J.; Lee, S. K. Influence of Atmospheric Plasma on Physicochemical Properties of Vapor-Grown Graphite Nanofibers. *J. Colloid Interface Sci.* **2005**, *285*, 306–313.
22. He, P.; Dai, L. M. Aligned Carbon Nanotube DNA Electrochemical Sensors. *Chem. Commun.* **2004**, 348–349.
23. Yun, Y. H.; Shanov, V.; Tu, Y.; Schulz, M. J.; Yarmolenko, S.; Neralla, S.; Sankar, J.; Subramaniam, S. A Multiwall Carbon Nanotube Tower Electrochemical Actuator. *Nano Lett.* **2006**, *6*, 689–693.
24. Mukai, K.; Asaka, K.; Sugino, T.; Kiyohara, K.; Takeuchi, I.; Terasawa, N.; Futaba, D. N.; Hata, K.; Fukushima, T.; Aida, T. Highly Conductive Sheets from Millimeter-Long Single-Walled Carbon Nanotubes and Ionic Liquids: Application to Fast-Moving, Low-Voltage Electromechanical Actuators Operable in Air. *Adv. Mater.* **2009**, *21*, 1582–1585.
25. Guo, W.; Guo, Y. Giant Axial Electrostrictive Deformation in Carbon Nanotubes. *Phys. Rev. Lett.* **2003**, *91*, 115501.
26. Xu, Y. X.; Bai, H.; Lu, G. W.; Li, C.; Shi, G. Q. Flexible Graphene Films *via* The Filtration of Water-Soluble Noncovalent Functionalized Graphene Sheets. *J. Am. Chem. Soc.* **2008**, *130*, 5856–5857.